UCLA
UCLA Previously Published Works

Title

Spatiotemporal Live-Cell Analysis of Photoreceptor Outer Segment Membrane Ingestion by the Retinal Pigment Epithelium Reveals Actin-Regulated Scission.

Permalink

https://escholarship.org/uc/item/3h69c4h6

Journal

The Journal of Neuroscience, 43(15)

Authors

Umapathy, Ankita

Torten, Gil

Paniagua, Antonio

et al.

Publication Date

2023-04-12

DOI

10.1523/JNEUROSCI.1726-22.2023

Copyright Information

Peer reviewed

Cellular/Molecular

Spatiotemporal Live-Cell Analysis of Photoreceptor Outer Segment Membrane Ingestion by the Retinal Pigment Epithelium Reveals Actin-Regulated Scission

Ankita Umapathy, Gil Torten, Antonio E. Paniagua, Julie Chung, Madeline Tomlinson, Caleb Lim, and David S. Williams

Department of Ophthalmology and Stein Eye Institute, and Department of Neurobiology, David Geffen School of Medicine at UCLA, Los Angeles, California 90095

The photoreceptor outer segment (OS) is the phototransductive organelle in the vertebrate retina. OS tips are regularly ingested and degraded by the adjacent retinal pigment epithelium (RPE), offsetting the addition of new disk membrane at the base of the OS. This catabolic role of the RPE is essential for photoreceptor health, with defects in ingestion or degradation underlying different forms of retinal degeneration and blindness. Although proteins required for OS tip ingestion have been identified, spatiotemporal analysis of the ingestion process in live RPE cells is lacking; hence, the literature reflects no common understanding of the cellular mechanisms that affect ingestion. We imaged live RPE cells from mice (both sexes) to elucidate the ingestion events in real time. Our imaging revealed roles for f-actin dynamics and specific dynamic localizations of two BAR (Bin-Amphiphysin-Rvs) proteins, FBP17 and AMPH1-BAR, in shaping the RPE apical membrane as it surrounds the OS tip. Completion of ingestion was observed to occur by scission of the OS tip from the remainder of the OS, with a transient concentration of f-actin forming around the site of imminent scission. Actin dynamics were also required for regulating the size of the ingested OS tip, and the time course of the overall ingestion process. The size of the ingested tip is consistent with the term "phagocytosis." However, phagocytosis usually refers to engulfment of an entire particle or cell, whereas our observations of OS tip scission indicate a process that is more specifically described as "trogocytosis," in which one cell "nibbles" another cell.

Key words: actin dynamics; BAR proteins; live-cell imaging; phagocytosis; RPE; trogocytosis

---

Significance Statement

The ingestion of the photoreceptor outer segment (OS) tips by the retinal pigment epithelium (RPE) is a dynamic cellular process that has fascinated scientists for 60 years. Yet its molecular mechanisms had not been addressed in living cells. We developed a live-cell imaging approach to investigate OS tip ingestion, and focused on the dynamic participation of actin filaments and membrane-shaping BAR proteins. We observed scission of OS tips for the first time, and were able to monitor local changes in protein concentration preceding, during, and following scission. Our approach revealed that actin filaments were concentrated at the site of OS scission and were required for regulating the size of the ingested OS tip and the time course of the ingestion process.

Introduction

The retinal pigment epithelium (RPE) is an extraordinary epithelium. It performs several specialized functions that are crucial to the maintenance of vision (Strauss, 2005; Lakkaraju et al., 2020). In one such function, it takes care of the catabolic phase of photoreceptor outer segment (OS) renewal. OSs are composed of tightly packed membranous disks, which contain the phototransductive proteins. The distal tip, amounting to ~10% of each OS in mammals, is phagocytosed by the RPE each day (Young, 1967; Young and Bok, 1969). Given that each RPE cell interfaces with numerous photoreceptors, >200 in the central mouse retina (Volland et al., 2015), it must ingest and degrade large amounts
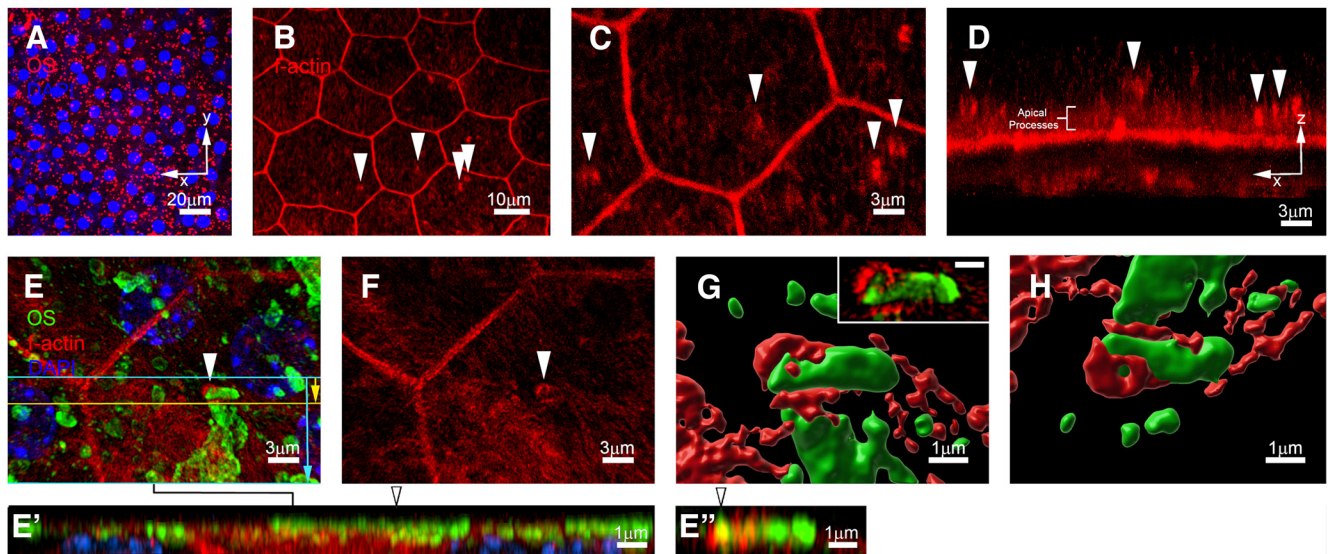
Figure 1. Labeling of f-actin-rich phagocytic cups in fixed flat-mounts of albino mouse RPE. *A*, RPE flat-mount collected after light onset and then fixed. It was labeled with antibodies against the N-terminal 4D2 epitope of rhodopsin (red) and DAPI to visualize nuclei (blue), demonstrating a high density of phagosomes. *B–D*, RPE flat-mount from fixed eyes that were collected before light onset. It was labeled with phalloidin-TRITC (red) to visualize actin filaments. The f-actin-rich, cup-like structures can be seen (white arrowheads) in *B* and, with higher magnification, in *C*. The flat-mount in *D*, reconstructed in the apical–basal axis, instead of en face as in *A–C*, shows the stronger phalloidin labeling of the cups relative to the apical processes. *E*, *F*, RPE flat-mount from fixed eyes that were collected before light onset. It was labeled with phalloidin-TRITC (red) to visualize actin filaments and antibodies against the N-terminal 4D2 RHO epitope (green). An f-actin-rich cup (white arrowhead) can be seen wrapped around an end of an OS in an en face view. *E'*, *E''*, Orthogonal projections of *E*, showing the apical–basal axis. The black-bordered arrowheads indicate the same position along the *x*-axis, as shown by the white arrowhead in both *E* and *F*. *E'*, A *y*-axis projection extending between the two cyan lines and along the complete *x*-axis. This view shows that nearly all the RHO labeling is at the apical surface. Particularly, because these flat-mounts were fixed before detaching the neural retinas, we suspect that much of the RHO labeling represents OS distal fragments that may have ripped off from the retina when it was detached; and the majority of the OS tips were not associated with an f-actin cup at the time of fixation of the intact retina. *E''*, A *y*-axis projection extending only to the yellow line (from the top cyan line) and including only the region of the *x*-axis that is shown in *G* and *H*. *G*, *H*, The cup indicated by white arrowhead in both *E* and *F* was 3-D rendered using the Surfaces tool in Imaris. The en face view (*G*) and the horizontally 180° rotated view (*H*) of the underside of the cup are shown. *G*, Inset, A higher magnification of the fluorescence image, corresponding to the central area of the Imaris rendering. Scale bar, 1 µm.

of disk membranes daily. Moreover, RPE cells are largely postmitotic, so that they are required to perform this process over the lifetime of the organism.

Phagocytosis was first studied and is best known in the context of innate immunity (Lim et al., 2017). OS membrane ingestion and degradation by the RPE shares some similarity to the phagocytosis of pathogens by neutrophils and macrophages, but its role requires unique adaptations. Defects in OS membrane ingestion and degradation by the RPE are linked to retinal degenerations and thus blindness. Impaired ingestion results in photoreceptor degeneration (Gal et al., 2000) and inefficient degradation leads to the accumulation of lipid-containing deposits (Rakoczy et al., 2002; Wavre-Shapton et al., 2013; Jiang et al., 2015; Notomi et al., 2019), which contribute to progressive retinal disease, especially macular degeneration, a common disorder among the elderly (Pikuleva and Curcio, 2014).

The initial stage of ingestion of an OS tip involves binding to the RPE apical surface, which is facilitated by the integrin $\alpha v \beta 5$ (Finnemann et al., 1997). The MER tyrosine kinase (MERTK) receptor is required for actual ingestion (Gal et al., 2000; Mazzoni et al., 2014). Expansion of the apical RPE membrane in close apposition to the membrane of the OS tip appears to precede ingestion; importantly, this membrane expansion was distinct from the more permanent apical processes (Steinberg et al., 1977; Nilsson, 1978; Chaitin and Hall, 1983; Matsumoto et al., 1987). The membrane expansion requires activation of the Rac1 GTPase and reorganization of the f-actin cytoskeleton (Mao and Finnemann, 2012) and involves dynamic protruding sheets of membrane (Jiang et al., 2015; Almedawar et al., 2020) that form a cup around the OS tip.

Although these and other molecular events involved in OS tip ingestion have been identified, and models of this dynamic process have been proposed, the process has been studied almost exclusively with fixed cells or tissues. Hence, it is not known how molecules are spatially and temporally coordinated to effect ingestion. Static visualizations of the phagocytic cup, though informative, cannot provide a complete understanding of a process that is inherently transient and dynamic; fixed tissue cannot provide a sequence of rapid events, or the opportunity to observe or interpret the significance of transient structural changes and protein localization. To address this shortcoming, we report here on the first live-cell analysis of molecular components involved in RPE ingestion of OS membranes. We have focused on the involvement of actin filaments and Bin-Amphiphysin-Rev (BAR) proteins in the expansion of the apical RPE membrane to form a cup around the OS tip and the ensuing scission of the OS to effect the final stage of ingestion.

Materials and Methods

Animals. All procedures conformed to institutional animal care and use authorizations. HSD Non-Swiss albino mice (Harlan Laboratories) and CD1 mice were kept on a 12 h light/dark cycle under 10–50 lux fluorescent light during the light cycle. The mice were randomized according to sex for the studies.

Immunofluorescence of phagosomes and f-actin. Albino mouse eyes were collected before light onset, fixed for 10 min at room temperature (RT) by immersion into buffered 4% formaldehyde, and dissected into eyecups. The neural retina was removed, and the remaining RPE/choroid/sclera was flat-mounted and fixed for an additional 50 min at RT. The flat-mounts were then washed in PBS and incubated with blocking solution (5% normal goat serum, 1% BSA, 0.25% Triton X-100 in PBS, pH 7.4) for 1 h at RT. They were then incubated with primary antibodies
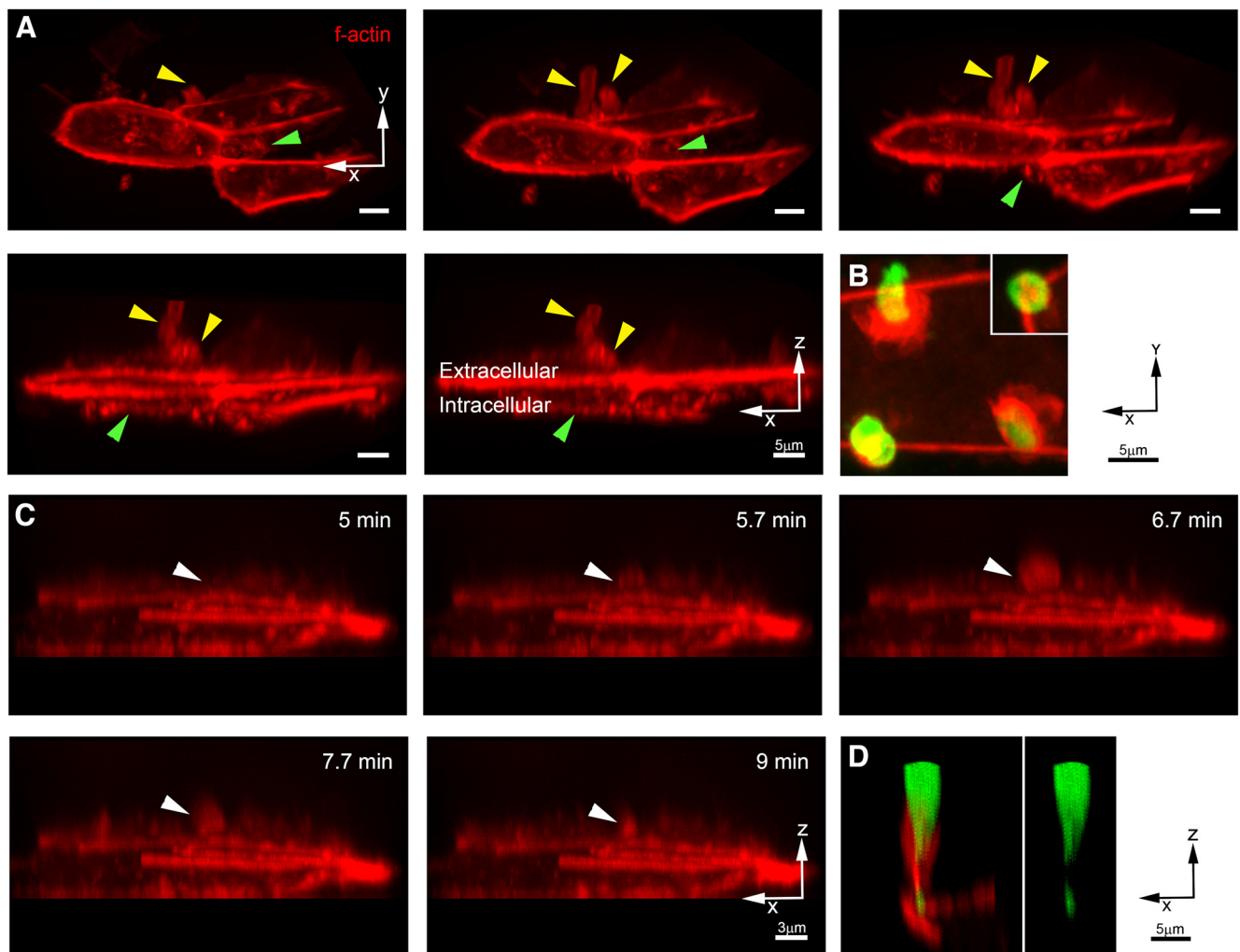
Figure 2. Transfection of cultured primary mouse RPE cells with F-Tractin-RFP. ***A***, Rotation of still image. The circumferential ring of f-actin (red) is evident in all 4 cells, as are the basal infoldings (green arrowheads), and, after the addition of OSs (data not shown), apically extending cups were evident (yellow arrowheads). The basal and apical protrusions can be seen as the field of view is gradually rotated from an en face *X–Y* orientation (far left image, top row) to an *X–Z* orientation (second image, second row). ***B***, En face (*X–Y*) view of part of a cell, showing four areas (including the inset) where f-actin-rich protrusions have formed beneath a bound OS (green). The actin cup in the inset (top right) is shown in *X–Z* reconstruction in ***D*** and Movie 1. The red lines represent the apical circumferential actin that outlines the cell boundary. ***C***, Time-lapse images from live-cell imaging, shown in *X–Z* reconstruction, using spinning disk confocal microscopy. f-Actin is also evident in transient membrane ruffles (white arrowheads) that protruded apically above the f-actin ring (first two panels), blossomed into crater-like cups (e.g., third panel), which then collapsed, all within a time period of 4 min. ***D***, *X–Z* reconstruction of the OS (green) and the f-actin (red) associated membrane cup that is shown in *X–Y* view, in the inset, top right in ***B***. This image is from the first frame of Movie 1. It shows an OS fragment that has just been separated from the end of the OS. In the left panel, a high-intensity image of F-tractin labeling, indicating a high concentration of f-actin, can be observed in the region between the separated fragment and the rest of the OS. The right panel shows the OS and the OS fragment without actin labeling. Note that the imaging for this figure was performed on the older spinning disk confocal system, which resulted in artifactual stretching in the z-axis; this stretching has not been corrected by ad hoc compression. All other figures in the present article include imaging performed on the newer system (see Materials and Methods), with which there was minimal distortion in the z-axis.

against rhodopsin (RHO; mouse RHO mAb4D2, 1:2000) overnight at 4°C in PBS containing 1% BSA. Following thorough washes in PBS containing 0.1% BSA, cells were incubated with an Alexa Fluor-conjugated secondary antibody (488), DAPI to visualize nuclei, and phalloidin-TRITC to visualize f-actin, for 1 h at RT, and mounted with FLUORO-GEL with Tris Buffer (Electron Microscopy Sciences). Cells were imaged using a Zeiss Airyscan with Zen Blue software, or a NIKON SIM system.

Cell culture. RPE primary cells were isolated from mouse retinas as described previously (Gibbs et al., 2003; Gibbs and Williams, 2003). In brief, intact eyes were removed from 8- to 15-d-old mice, washed in growth medium [GM; DMEM with GlutaMax (high glucose) and MEM nonessential amino acids], and incubated with 2% (w/v) dispase in GM for 45 min at 37°C. The eyes were then washed three times in GM supplemented with 10% fetal bovine serum (FBS), 1% penicillin/streptomycin, and 1× HEPES. After removal of the anterior tissues including the cornea, iris-pigmented epithelium, and lens, the posterior eyecups were incubated in GM with FBS and HEPES for 20 min at 37°C. The neural retina was then removed, and intact sheets of RPE were peeled off from

Bruch's membrane, washed, and then cultured in GM with FBS (excluding HEPES). All the reagents were from Thermo Fisher Scientific, unless otherwise specified. For live-cell imaging, cells were cultured and imaged in eight-well cover glass chambers (LABTEK, Thermo Fisher Scientific) or 10 mm microwell-containing 35 mm glass-bottom Petri dishes (#1.5 glass, 0.16–0.19 mm; MATTEK) in the appropriate GM. All cells were maintained at 37°C with 5% CO_2 for a maximum of 5 d; cells can be cultured for at least 5 d without compromising their differentiated phenotype or phagocytic ability (Gibbs et al., 2003; Gibbs and Williams, 2003).

Expression of tagged proteins. Cells were transfected with the plasmid constructs on day 2 or 3 following plating, using either jetPRIME (Polyplus) or Lipofectamine 3000 (Thermo Fisher Scientific). The F-Tractin-RFP and F-Tractin-GFP (gifts from Michael Schell, Uniformed Services University, Bethesda, MD) plasmids contain the f-actin binding domain of rat ITPKA (inositol-triphosphate 3-kinase A) fused to monomeric EGFP, described in the study by Johnson and Schell (2009), or tdTomato, both on the C terminus. Plasmids pEGFP-C1-FBP17 and pCAG-AMPH1-BAR-mCherry (BAR domain of human amphiphysin-1;

amino acids 1–256), C-terminally tagged with mCherry) were all obtained from Addgene; pEGFP-C1-FBP17 was a gift from Pietro De Camilli, Yale School of Medicine, New Haven (plasmid #22229, Addgene; Itoh et al., 2005); pCAG-AMPH1-BAR-mCherry was a gift from Tobias Meyer, Weill Cornell Medicine, New York (plasmid #85130, Addgene; Hayer et al., 2016). All constructs were sequenced using the appropriate primers to confirm identity before use.

OS isolation. OSs were isolated from mice that were dark adapted overnight, using an OptiPrep (Sigma-Aldrich) step gradient (Hazim and Williams, 2018) or a Percoll continuous gradient (Williams et al., 1989). Briefly, retinas were removed and placed in 1 ml of Ringer's solution (130 mM NaCl, 3.6 mM KCl, 2.4 mM MgCl$_2$, 1.2 mM CaCl$_2$, 0.02 mM EDTA, and 10 mM HEPES, adjusted to pH 7.4), with a maximum of 20 retinas/gradient, on ice, under infrared illumination, and homogenized with five strokes in a glass pestle. After brief centrifugation (100 × g, 1 min), the supernatant was loaded on the top of an OptiPrep or a Percoll gradient. The OptiPrep step gradient contained 3 ml steps of 8%, 10%, and 15% OptiPrep in Ringer's solution, in 14 ml polypropylene centrifuge tubes. The tubes were centrifuged for 20 min at 8500 rpm at 4°C in a swinging bucket rotor (model HB-6, Sorvall) with slow acceleration and deceleration. OSs were collected from the 10–15% interface, diluted threefold with Ringer's solution, and centrifuged at 10,000 × g for 10 min at 4°C, and the resulting OS pellet was resuspended in Ringer's solution. OS isolation on preformed 65–30% Percoll gradients followed that described for rat OSs previously (Williams et al., 1989). The concentration of intact OSs was determined with a hemocytometer under phase microscopy. OSs were then either used fresh or pelleted and aliquoted to be stored at −80°C in DMEM/2.5% (w/v) sucrose until needed. For live-imaging experiments, OSs were labeled with 0.05 mg/ml fluorescent dyes (Alexa Fluor 488, 594, or 647 succinimidyl esters) for 25–30 min at 4°C in 0.1 M NaHCO$_3$, at pH 8.4. OSs were washed three times with Ringer's solution by centrifuging at 10,000 × g for 5 min. The final pellet was resuspended in primary RPE GM.

OS ingestion by primary RPE cells. Primary RPE cells on glass-bottomed imaging slides or dishes were incubated at 17°C for 30 min to equilibrate cells to the lowered temperature and pulsed with 300 μl (slide) or 150 μl (dish) prelabeled OS suspension in media (10^7 OSs/ml) for 1 h at 17°C. Cells were then washed three times with GM and immediately imaged for up to ~90 min (during the chase period), using spinning disk confocal microscopy. Cells used in the cytochalasin D experiments were pretreated with 1 μM cytochalasin D (or DMSO only) for 25 min and pulsed for 20 min at 37°C (instead of 17°C) with labeled OSs, in the presence of the drug (or DMSO only). This experimental paradigm was necessary as inhibition, established during pretreatment at 37°C, was weakened when cells were pulsed with OSs and drug at 17°C. Cytochalasin D was immediately removed when the OSs were washed off, and therefore not included during live imaging to allow resumption of actin polymerization. Cytochalasin D was purchased from Sigma-Aldrich (10 mM stock solution prepared in 100% anhydrous DMSO).

Imaging of OS ingestion. 3-D imaging was performed using one of the following two spinning disk confocal microscope systems available to us. (1) An UltraVIEW ERS (PerkinElmer) containing an Axio Observer.A1 inverted microscope (Carl Zeiss) fitted with an environment chamber maintained at 37°C for at least 1 h before imaging and supplied with 5% CO$_2$. Time-lapse 3-D movies (step size, 1 μm) were acquired with a 63× numerical aperture (NA) 1.4 oil objective using Volocity software (PerkinElmer) and an EMCCD camera (model C11440-22CU, Hamamatsu Photonics) for a duration of 10 min with 30 s intervals in the relevant channels using sequential imaging. (2) A Yokogawa CSU-X1 10,000 rpm disk (https://www.yokogawa.com/us/solutions/products-platforms/life-science/spinning-disk-confocal/csu-x1-confocal-scanner-unit/) was installed on a Nikon Eclipse Ti2-E inverted microscope fitted with an environmental stage top incubator (Tokai Hit), maintained at 37°C, and supplied with 5% CO$_2$. 3-D movies (step size, 0.5 μm) were acquired using a Mad City Labs Piezo Z stage-top insert with a 60× Plan Apo λ NA 1.4 objective with NIS-Elements software (Nikon). Images were acquired with Andor 888 Back Illuminated EMCCD cameras split via an Andor TuCam dual-emission splitting component, typically at 20 s intervals. Movies from vehicle (DMSO) or
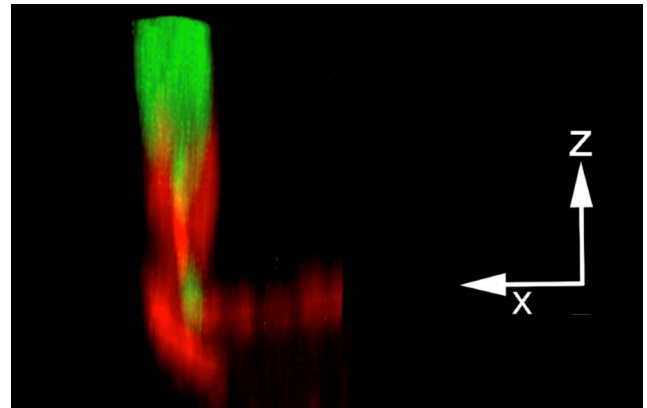
Movie 1. Live-imaging of ingestion of an Alexa Fluor 488 dye labeled OS fragment (green) by a primary mouse RPE cell transfected with F-Tractin-RFP (f-actin, red). The movie shows an *X–Z* orientation, from 3-D reconstruction of stacks of images in the *X–Y* orientation, obtained by stepping through the z-axis. Images were obtained on the older spinning disk system, with which there is resulting distortion in the z-axis. The first frame (also in Fig. 2D) shows an OS fragment that is separated from the rest of the OS by an intense concentration of actin filaments. As the movie proceeds, a second fragment is separated from the OS. This fragment moves down the actin cup as the rest of the OS appears to be released from the cup. The movie plays at 5 frames/s. Each frame was acquired every 30 s over 10 min, so that the playback rate is 150 times the acquisition rate. Scale bar, 4 μm. [View online]

cytochalasin D-treated cells were imaged under identical conditions. Note that the Ultraview system was significantly older, and live images from this system were artifactually stretched in the z-axis. This stretching, which was evident following 3-D reconstruction, was not corrected by any *ad hoc* compression. Imaging obtained with the Ultraview system is shown only in Figure 2 and Movie 1.

3-D modeling. Movies were imported into the Imaris software from the Volocity or Nikon Elements software. Channel alignment was corrected, as needed, using Tetraspeck beads. The "Surfaces" function of Imaris was used to manually create renderings that faithfully reflected the fluorescence intensities of the raw movie, as much as possible. Renderings were performed to illustrate the dynamic characteristics of each phagocytic event more clearly than in the raw fluorescence movies.

pSIVA labeling. Mouse eyes were enucleated immediately after death, and the neural retinas were dissected from the posterior eyecup. Following a previously published method (Ruggiero et al., 2012), retinas were incubated with 10 μg/ml CellMask stain in Hanks buffered saline (HBS) for 10 min at 37°C, and then with 10 μg/ml using pSIVA REAL-TIME Apoptosis Fluorescent Microscopy Kit (pSIVA; catalog #APO004, BIO-RAD) in HBS for 5 min at 37°C. The unfixed retinas were then placed on glass slides, with the photoreceptor side up, and imaged with a laser-scanning confocal microscope (model FV1000, Olympus) 15–30 min after enucleation. Crude or purified OSs were incubated in HBS with 5 μg/ml CellMask and 15 μg/ml pSIVA for 30 min on ice. They were then centrifuged at 10,000 × g, resuspended in HBS, and imaged on glass slides.

Experimental design and statistical analysis. Phagosome diameter was measured in the *x*- and *y*-dimensions, using Imaris. Only phagosomes that had resulted from an observed scission event were included for analysis. The length of time for the ingestion of an OS tip was measured from the formation of a membrane cup around the OS tip until the completion of the first scission event, or the passage of 10 min, whichever occurred sooner. Measurements of the time taken for ingestion and the phagosome diameter from DMSO-only and cytochalasin D-treated cells were analyzed using a two-tailed Wilcoxon rank-sum test. Data are shown as scatter plots; *n* and *p* values are shown in the figure legends.

Results

Visualization of actin filaments in the RPE
We first imaged structures and specific protein localization in freshly dissected RPE flat-mounts collected from albino mice,
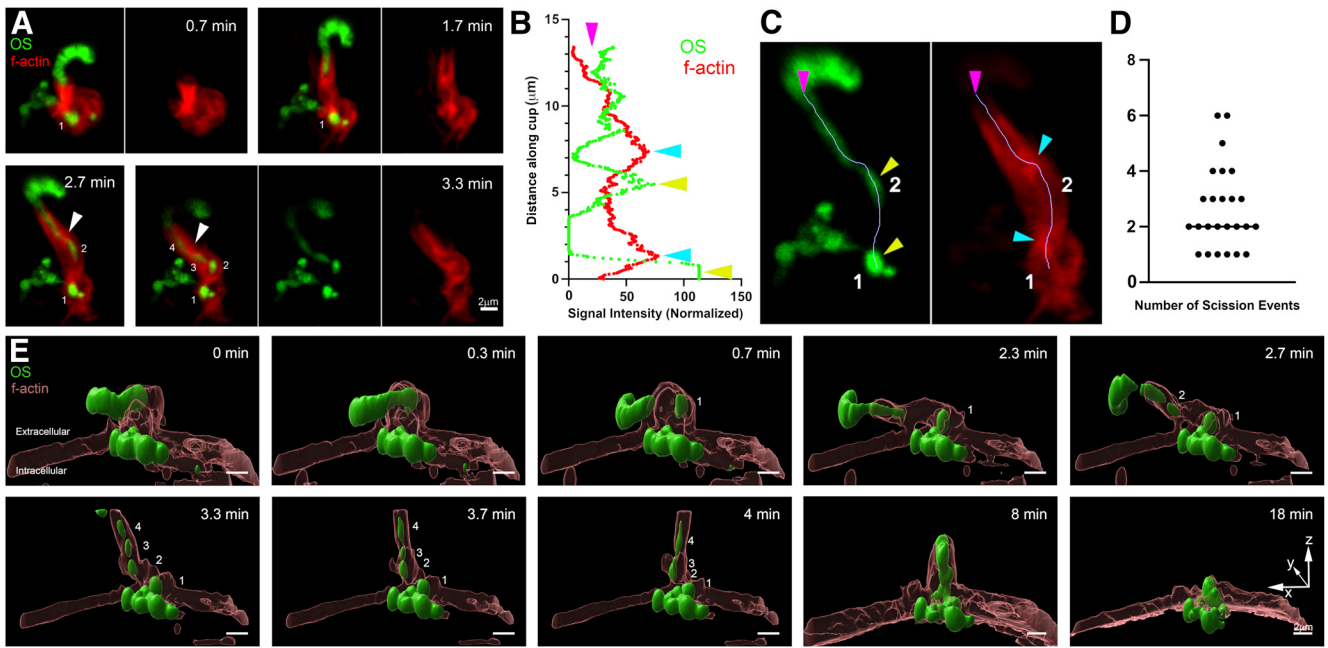
Figure 3. Dynamic localization of f-actin within the phagocytic cup. **A**, Selected frames taken from Movie 2. Primary mouse RPE cells were transiently transfected with F-Tractin-RFP (f-actin, red) and fed Alexa Fluor 488 dye-labeled isolated OSs (green). The images are from 3D reconstructions and are all shown in a similar orientation, which approximates the long axis of the cup and the OS. Following ensheathment of the end of an OS by an f-actin-associated cup, the first phagosome (labeled 1) is evident below intense f-actin labeling (0.7 min). Three additional phagosomes (labeled 2, 3, and 4) are formed by 3.3 min, as the cup unsheathes more of the OS. Formation of the phagosomes coincides with an increase in f-actin intensity at the site of scission (e.g., white arrowheads). **B**, Intensity plot of the OS and f-actin signals at the 2.7 min time point. **C**, Images of the 2.7 min time point, showing the OS and f-actin signals separately; the lines along the OS and cup track where the intensity signals were measured. The pink arrowheads represent the top of the intensity measurement, and the yellow and cyan arrowheads indicate peaks in the OS and f-actin labeling intensities, respectively. A distinct f-actin intensity peak is associated with a decrease in OS signal (i.e., where the OS has been "pinched" during the scission process). **D**, The number of scission events observed in a phagocytic cup in different 10 min movies. Each datum represents a single phagocytic cup ($n = 25$), each from a separate cell culture. **E**, Selected frames from the Imaris Surfaces rendering of Movie 3. The 0.7, 2.7, and 3.3 min timepoints correspond to three of the frames in **A**.

after light onset, when phagosome density is highest (LaVail, 1976; Besharse and Hollyfield, 1979; Fig. 1A). Clear phalloidin labeling indicates the circumferential ring of f-actin, associated with cell–cell junctions (Fig. 1B,C). More apically, among the more lightly labeled f-actin of the apical microvilli, concentrations of phalloidin label represent f-actin associated with the formation of membrane cups (Fig. 1B–F, arrowheads). 3-D rendering (Imaris Surfaces) indicates the close association between f-actin underlying the RPE apical membrane and an OS tip (Fig. 1G,H). However, studies of fixed tissue are of limited use for understanding actin dynamics. Moreover, the mechanical separation of the retina from the RPE, which is required to prepare the flat-mount, often resulted in phagocytic cup-like structures that did not contain OSs. Therefore, for a more detailed analysis of OS phagocytosis and, importantly, the opportunity to introduce temporal resolution, we used a live RPE cell model to emulate the process.

We used mouse primary RPE cells, which we found to be tractable, especially with respect to transfection efficiency and the timing of OS ingestion. To enrich for ingestion events, cells were first incubated with isolated mouse OSs at 17°C, as the cooler temperature permits binding but prevents significant ingestion of OSs (Hall and Abrams, 1987). After this incubation, excess unbound or loosely bound OSs were washed away, and the cells were incubated at 37°C to initiate synchronized ingestion.

Transient transfection of primary RPE cells with F-Tractin-RFP resulted in a pattern that was similar to phalloidin labeling, with localization (1) to the circumferential f-actin ring (Fig. 2A); (2) in dynamic structures at the basal RPE, likely the basal infoldings (Fig. 2A, green arrowheads; Bonilha et al., 1999); (3) within
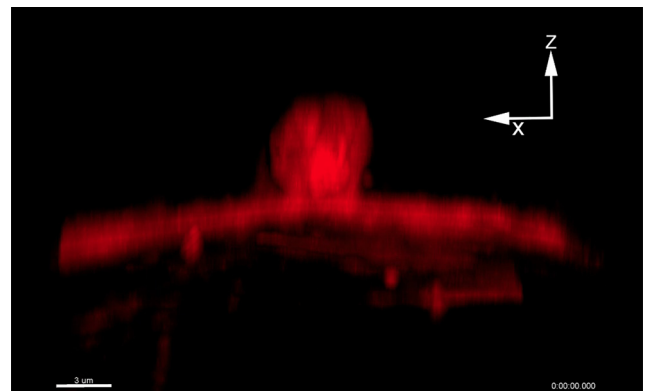
Movie 2. Live imaging of progressive ingestion of the end of an OS, labeled with Alexa Fluor 488 dye (solid green), by a primary mouse RPE cell transfected with F-Tractin-RFP (red; Fig. 3A, time-lapse series). A series of scission events results in the ingestion of several OS fragments. The movie steps through each frame at 3-D orientations that best demonstrate the dynamic localization of f-actin in the cup. It begins in an X–Z orientation, showing only f-actin labeling. It then rotates toward an X–Y orientation. After 10 s of movie play time (not the timer in the field of view), the z-planes beneath the cup, including those containing the f-actin ring, were hidden for better contrast of the changing f-actin localizations within the cup. After 14 s of play time, the scene is tilted back and forth to provide a better 3-D view of the elongating cup. After 24 s of play time, the movie is paused, and the scene is rotated back to an X–Z orientation. Figure 3 shows a series of time-lapse images from this movie, although the images in the figure are all in a similar orientation, which represents a rotation from the X–Z orientation toward an X–Y orientation. [View online]

transient membrane ruffles that curved into crater-like cups but quickly collapsed (Fig. 2C, white arrowheads); and (4) in apical extensions that formed around part of an OS when OSs were added (Fig. 2A, yellow arrowheads; OSs were not labeled here).

Figure 2*B* shows an en face view of OSs (green), associated with f-actin-rich apical extensions (red) from the RPE cell.

Scission and ingestion

Following incubation with OSs, ingestion events were observed for up to 90 min. Peak activity occurred in the first 30–45 min. An average of two to three ingestion events typically occurred at different locations on a given cell.

In the first experiments, we performed live-cell imaging on an older spinning disk confocal system. 3-D reconstruction with this system resulted in artifactual stretching in the *z*-axis. Nevertheless, F-Tractin labeling of actin filaments, associated with membrane cups, was evident as it extended above the circumferential f-actin and enclosed around the end of each OS. Following envelopment of the end of an OS by the extended actin filaments, the enveloped end of the OS separated from the rest of the OS as it became engulfed by the RPE cell. During this process, a high density of actin filaments was evident at the point of scission; in Figure 2*D*, intense F-Tractin labeling is evident at the point between the OS and the separated fragment. As shown in Movie 1, the engulfment of a second fragment may follow. The engulfed OS fragments descend into the cell, and the apical extensions of the f-actin cup subsequently retract (Movie 1). The intimate proximity of the f-actin cup with the tip of the OS, as it becomes detached, suggests a scission event involving dynamic actin filaments.

Using our method of OS isolation, the OSs remain largely intact, as cylindrical structures, during the initial period of observation. Commonly, we observed multiple sequential scission events, so that multiple phagosomes resulted from a single OS. Figure 3 shows live-cell fluorescence imaging of f-actin protrusions, representing an elongated cup, extending along an OS (here, a newer spinning disk confocal system was used). Scission events appeared to occur at fairly equal intervals along the OS, resulting in a tube containing several similarly sized phagosomes. In the example in Figure 3*A*, four discrete phagosomes are evident. Each scission event, leading to the formation of these phagosomes, is associated with a transient, increased intensity of F-Tractin labeling of actin filaments, at the site of the imminent scission. A signal intensity plot of the f-actin and the OS signals shows that increased f-actin concentration associates with decreased OS labeling (Fig. 3*B*,*C*). These observations indicate dynamic behavior of specifically localized actin filaments, functioning in detachment of packets of disk membrane from the OS tip (Movie 2). The median number of scission events that we observed per OS was two (Fig. 3*D*).

To clarify the scission of the OS to form a discrete phagosome, Imaris Surfaces software was used to generate defined renderings of the fluorescent f-actin and OS signals, whose transparency could be altered to better visualize overlapping features. This rendering of the fluorescence illustrates scission events occurring within ~20 s; phagosome 1 forms between 0.3 and 0.7 min, and phagosome 2 forms between 2.3 and 2.7 min (Fig. 3*E*, Movie 3). The identification of scission events within the cup indicates that the process of OS membrane ingestion should be regarded more specifically as trogocytosis (Bettadapur et al., 2020; Freeman and Grinstein, 2021; see Discussion).

Inhibition of actin polymerization slows ingestion and reduces phagosome size

To test the requirements for actin filaments in membrane formation, mediating OS scission and tip ingestion, we inhibited actin
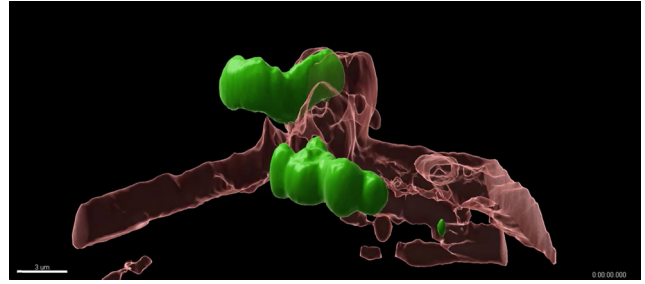
Movie 3. Live imaging rendered to provide 3-D perspective of progressive ingestion of the end of an OS, labeled with Alexa Fluor 488 dye (solid green), by a primary mouse RPE cell transfected with F-Tractin-RFP (reddish brown; Fig. 3*E*, time-lapse series). The *z*-axis is vertical. The movie plays at 5 frames/s. Each frame was acquired every 20 s, so that the playback rate is 100 times the acquisition rate. The movie shows 4 min of imaging (played back in 6 s). [View online]

polymerization. Although continuous exposure to 1 μM cytochalasin D did not affect OS binding to the RPE cell surface, it prevented any cup formation (Fig. 4*A*,*B*). We therefore used a more moderate treatment, whereby cells were treated with 1 μM cytochalasin D only during the prepulse and pulse periods (i.e., until the removal of the unbound OSs). During recovery from this treatment, membrane cups formed (Fig. 4*A*,*B*), but, initially, it is expected that there would have been more short actin filaments and actin network fragments (Schliwa, 1982), thus potentially affecting the dynamics of the f-actin network around the cup. Live-cell imaging, performed during this period of recovery from cytochalasin D treatment, revealed delayed cup formation. New scission events still occurred simultaneously with localized increases in f-actin intensity at the site of scission (Fig. 4*C*, white arrowheads; 10.7 and 14.3 min), suggesting that, at least in general terms, the scission mechanism appeared unaffected. However, the time taken between cup formation and completion of the first scission event was considerably longer following cytochalasin D treatment (Fig. 5*A*). Retarded ingestion was also evident by the longer interval between the formation of consecutive phagosomes from the same OS. For example, in the cytochalasin D-treated cell shown in Figure 4, phagosome 2 is evident at 5 min, but phagosomes 3 and 4 are not distinct until 6–7 min later (11–12 min panels) and 9 min later (14.3 min panel), respectively. In contrast, in the untreated cell, shown in Figure 2, phagosome 2 is evident at 2.7 min, and phagosomes 3 and 4 are evident just 40 s later (3.3 min panel).

The slower pace with which ingestion progressed between multiple scission events provided greater detail of the process (Fig. 4*C*, Movie 4). In untreated cells, a spot of concentrated f-actin remained visible above the new phagosome after scission and as the phagosome was distanced from the OS (Fig. 3*A*, note the high density of f-actin above phagosome 1 at 1.7 and 2.7 min). A high concentration of f-actin appeared to be contributing to the movement of the phagosome into the RPE cell. This behavior appeared exaggerated when cells were treated with cytochalasin D. In these cases, the spot of concentrated f-actin more clearly appeared to "follow" the nascent phagosome as it descended into the RPE cell, as if pushing the nascent fragment out of the cup and into the cell. For example, in Figure 4*C*, follow the f-actin intensity above phagosome 3, from the 11 and 12 min frames, where the phagosome is indicated by yellow arrowheads, to the 14.3 and 15 min frames. Movie 4 also illustrates this point and provides a sense of descending motion. These data suggest that actin dynamics may also be involved in the initial basal movement of phagosomes into the cell.
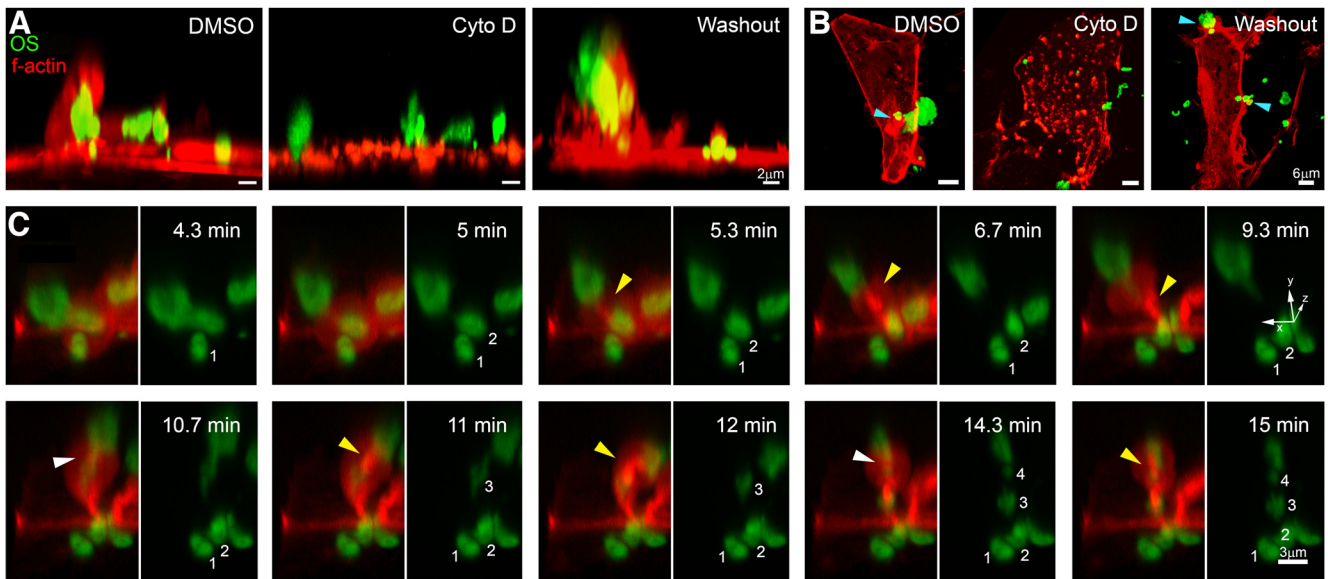
Figure 4. Effect of cytochalasin D pretreatment on the dynamic f-actin localization during ingestion. **A**, Phagocytic cups from RPE cell cultures treated with only DMSO (vehicle for cytochalasin), with 1 μм cytochalasin D for 45 min, or with cytochalasin D for 45 min plus an additional 1 h incubation after the cytochalasin D had been washed out. **B**, En face views of cells treated as in **A**. Cyan arrowheads indicate phagocytic cups. **C**, Selected frames taken from Movie 4. Primary mouse RPE cells were transiently transfected with F-Tractin-RFP (f-actin, red) and fed Alexa Fluor 488 dye-labeled isolated OS (green). Cells were pretreated with 1 μм cytochalasin D for 45 min at 37°C; during the last 20 min, they were incubated with OSs. Before imaging, cells were washed to remove unbound OSs and placed in medium lacking cytochalasin D. In the first panel (4.3 min), a single f-actin-rich cup has enveloped a portion of an OS, and one OS fragment is already contained within the RPE cell (labeled as "1"). By the second frame (5 min), scission to form a second phagosome (labeled 2) is complete. Over the next 10 min, 2 additional phagosomes (labeled 3 and 4) are generated from the partially enveloped OS. New scission events were observed as slightly localized increases in f-actin intensity, and a constriction of the cup rim, at the site of scission (white arrowheads, 10.7 and 14.3 min). Strong f-actin intensities (yellow arrowheads) are maintained after scission and appear to follow the excised OS fragment toward the interior of the cell (5–9.3 and 11–14.3 min), as if pushing the nascent fragment out of the cup and into cell; this motion is more evident in Movie 4.
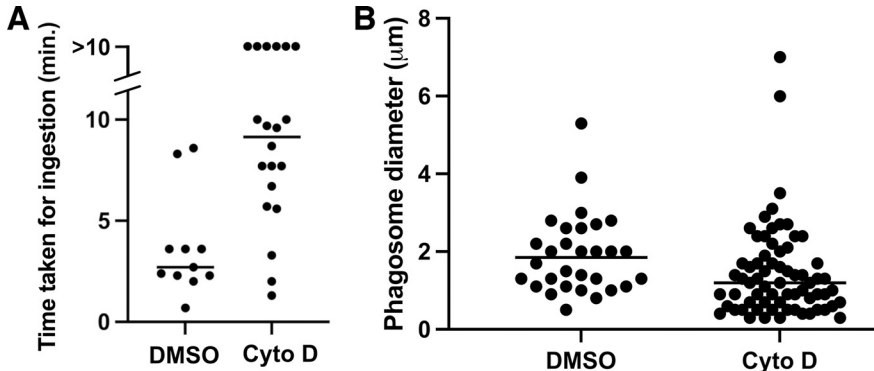
Figure 5. Actin dynamics play a role in determining the rate of OS tip ingestion and the size of that ingested. **A**, Time taken between the formation of a membrane cup around the OS tip and the completion of the first scission event. Each datum represents a single phagocytic cup within a 10 min movie (DMSO, $n = 11$; cytochalasin D, $n = 20$), with each movie from a separate cell culture. Complete scission did not occur within 10 min in some cytochalasin D-treated cells because of slower ingestion kinetics; these data are plotted as >10. **B**, Diameters of phagosomes (measured in the X–Y plane) formed in cytochalasin D-treated RPE cells versus cells treated with DMSO only (DMSO, $n = 30$; cytochalasin D, $n = 68$), with data aggregated from 6 separate experiments. For both **A** and **B**, the median values for each set of data are indicated by a horizontal line; $p = 0.0015$ and $p = 0.005$ for **A** and **B**, respectively, using a two-tailed Wilcoxon rank-sum test.

In addition to slower kinetics of OS ingestion, the moderate inhibition of actin polymerization in cytochalasin D-pretreated cells resulted in phagosomes with smaller diameters than in control (untreated or DMSO vehicle-treated) cells (median, 1.2 vs 1.8 μm; Fig. 5B). The finding of smaller phagosomes in response to cytochalasin D treatment indicates that the RPE actin cytoskeleton contributes to determining the size of the resulting OS phagosome. The OS tips of freshly dissected, detached mouse retinas have been shown to stain with externally applied pSIVA, indicating a local region of externalized phosphatidylserine (PS; Ruggiero et al., 2012; Fig. 6A,B).

At the time of light onset, the pSIVA labeling extends ~1.5 μm from the tip, thus identifying the region that would be contained within one phagosome and suggesting that the PS exposure might define phagosome size. We were therefore interested in whether the OSs that we fed to the RPE cells contained a localized tip of externalized PS. We found that the pSIVA labeling of the OS tips, present in freshly isolated retinas, was maintained in a crude OS preparation, obtained from the supernatant of freshly isolated retinas after a brief vortex. However, after gradient purification, or, simply, further incubation of crude OSs, pSIVA labeling appeared to have dispersed over the entire OS (Fig. 6C,D); we found that a "cap" of pSIVA labeling was evident at either end in only 3.4% of gradient-purified OSs ($n = 264$), obtained from six separate experiments. It follows that the gradient-purified OSs that we fed to the RPE cells and imaged were highly unlikely to possess a localized cap of externalized PS at their tip. Therefore, actin dynamics in the RPE appears to determine phagosome size without requiring input from localized PS exposure.

Association of BAR domain-containing proteins with the phagocytic cup

To further our understanding of the shaping of the membrane cup that forms around the OS tip, we investigated the spatiotemporal relationship of BAR domain-containing proteins, such as
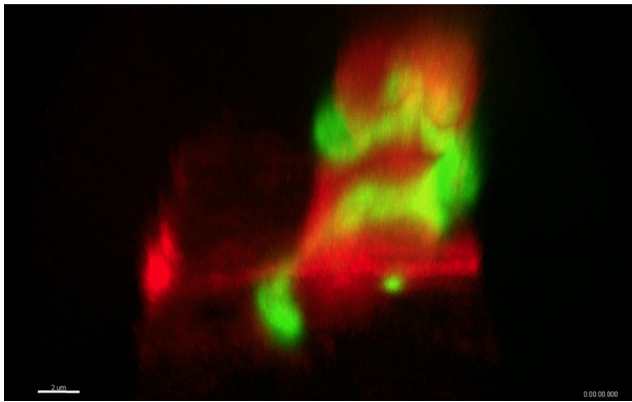
Movie 4. 3-D live imaging of the ingestion of an OS tip, following pretreatment of the RPE cell with 1 *μ*m cytochalasin D. OS material was labeled with Alexa Fluor 488 dye (solid green), and f-actin filaments are evident due to RPE cell transfection with F-Tractin-RFP (red). This movie plays at 5 frames/s; each frame was acquired every 20 s over a 20 min duration, so the playback rate is 100 times the acquisition rate. The frames are oriented between an *X*–*Y* and *X*–*Z* profile. Several phagocytic cups are evident. The cup on the left is shown in the time-lapse series in Figure 4*C*. A second cup on the right and a third behind the second are also evident. The cup on the left initially rotates clockwise as it extends to enclose and bite several phagosome-sized pieces from the whole OS. The localized increases in f-actin intensity at the cup rim coincide with new scission events. The concentration of f-actin then appears to persist and push the ingested OS fragment through the cup and into the cell. [View online]

formin-binding protein 17 (FBP17) and amphiphysin-1, over the course of OS tip ingestion. BAR proteins are divided into the following three subfamilies: classical/N-BAR, F-BAR, and I-BAR. FBP17 belongs to the F-BAR family, while amphiphysin 1 is an N-BAR protein. Both are intracellular proteins that have a crescent shape and bind to membranes through their concave face. F-BAR proteins tend to be less curved and more elongated compared with N-BAR proteins. Involvement of these membrane-associated BAR proteins has been shown in several cellular processes including clathrin-mediated endocytosis and phagocytosis; they sense and bind to areas of membrane curvature, while also being able to induce curvature (Stanishneva-Konovalova et al., 2016). They are also known to regulate actin dynamics by associating with key proteins such as actin nucleating factors (Itoh et al., 2005; Stanishneva-Konovalova et al., 2016). FBAR17 couples the plasma membrane and the actin cytoskeleton during cellular mechanoadaptation (Echarri et al., 2019). Yet, neither FBP17 nor amphiphysin-1 has been implicated previously in OS ingestion.

With live imaging, full-length EGFP-FBP17 appeared as discrete and transient patches at the plasma membrane of primary RPE cells. It was also invariably associated with membrane cups that contained OS tips (Fig. 7*A*, first panel). When cup extension was triggered through OS binding, FBP17 localized specifically to the rim of the cup (Fig. 7*A*, arrowheads in subsequent panels, Movie 5). If cup extension was halted and the cup regressed back into the cell, for example when an OS becomes unbound, FBP17 was lost from the rim (Fig. 7*A*, last panel, Movie 6).

It is also pertinent to note that unlike f-actin, which typically enriches at the site of scission and remains in place until the phagosome begins its descent into the cell, FBP17 did not localize to the apical membrane that enclosed the nascent phagosome (Fig. 7*A*, lower row, 6 min).

Compared with EGFP-FBP17, live-cell imaging of the BAR domain of amphiphysin-1 tagged to mCherry showed some similarities but also some differences. The AMPH1-BAR domain was also enriched at specific regions of the phagocytic cup; but it
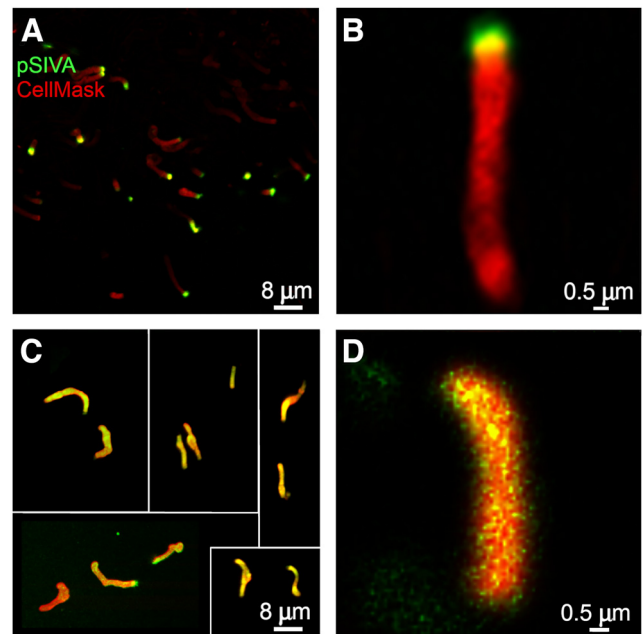
Figure 6. pSIVA labeling of mouse OSs, indicating external presence of PS. pSIVA labeling is green, and CellMask staining, which labels the entire plasma membrane, is red (yellow represents labeling by both). *A*, Freshly dissected, detached mouse retina; pSIVA label is restricted to many of the OS tips. *B*, Higher magnification of an OS from a preparation, such as that shown in *A*. *C*, Examples of gradient-purified OSs from different preparations. The bottom left panel shows two OSs with localized tip labeling by pSIVA, but the other OSs are labeled over most or all of their length. *D*, Higher magnification of a gradient-purified OS, labeled with pSIVA.

did not always colocalize with f-actin. In an extended cup, AMPH1-BAR localized strongly to the base of the cup, as well as at the rim, where FBP17 also localizes. AMPH1-BAR continued to localize at the base of the cup until the phagosome descended into the cell (Fig. 7, Movie 7).

Discussion

Here, we have provided a spatiotemporal analysis of OS membrane ingestion by RPE cells, an essential process in maintaining photoreceptor function and viability. Our focus has been on the dynamics of the actin cytoskeleton and the involvement of BAR proteins in OS membrane ingestion. To resolve these events, we followed proteins during high-speed 3-D imaging of primary RPE cells to a level that had not been achieved previously. Moreover, our studies challenged these primary cultures with OSs. Although this approach is technically more difficult than using a cell line with inert objects, such as beads, as the target of ingestion, it mimics the *in vivo* condition more closely than most previous phagocytosis studies. It has been shown that the phagocytic behavior of primary macrophages differs from that of macrophage-like cell lines (Barger et al., 2022), and the content of ingested material can have significant effects on the phagocytic process (Esteve-Rudd et al., 2018).

Following association between an OS and the RPE surface, which has been shown to involve adhesion by $\alpha_V\beta_5$ integrin (Finnemann et al., 1997), we observed that actin-based protrusions extend from the RPE cell to envelope the tip of the OS. The protrusion of the apical RPE membrane appears to play an active role in the removal of the OS tip. Early electron microscope studies were inconclusive about the basic mechanism of OS tip removal. These studies, which were limited to a 2-D perspective of fixed
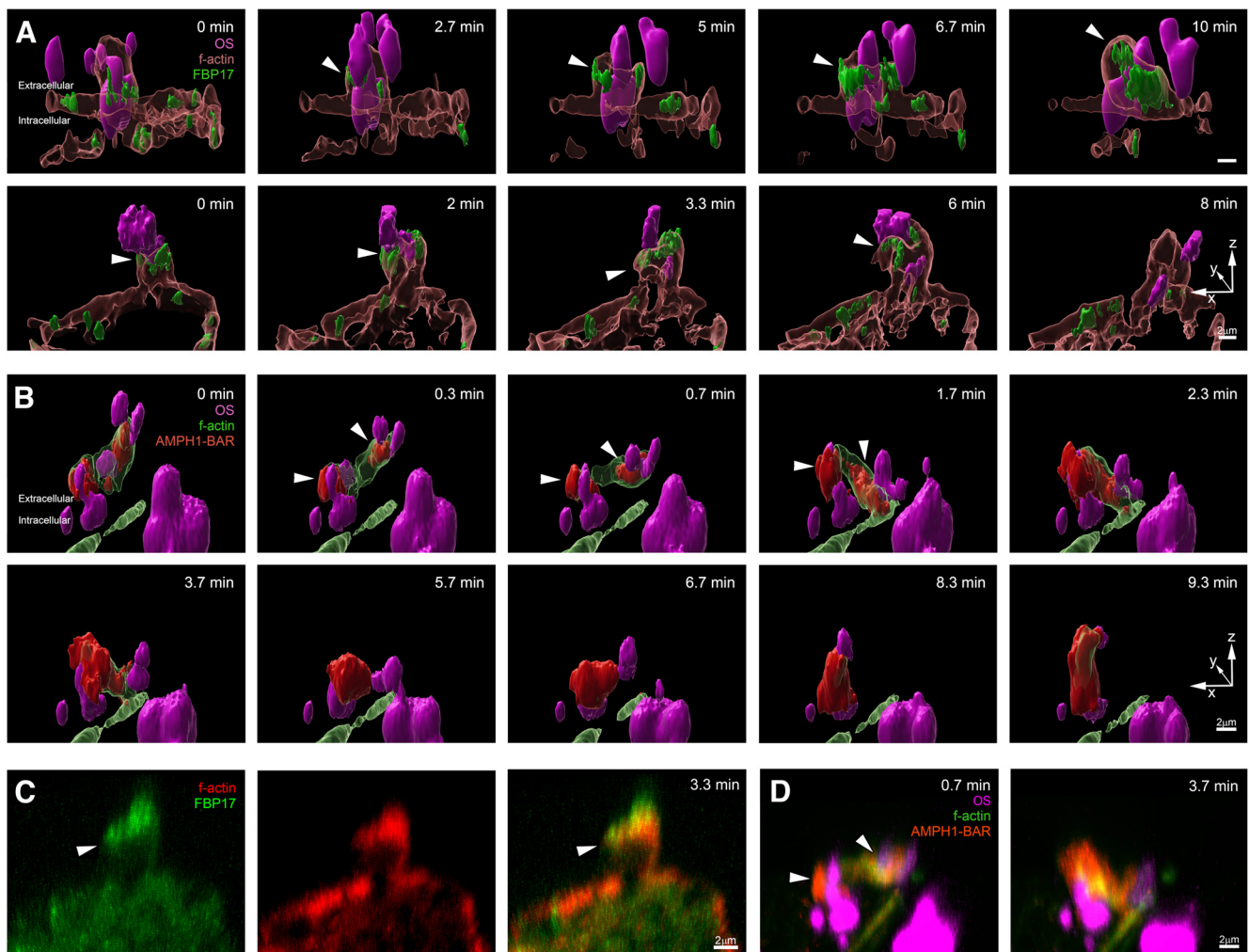
Figure 7. FBP17 and AMPH1-BAR localize to distinct curved membranes within the phagocytic cup. **A**, **B**, Imaris Surfaces renderings. **A**, Primary mouse RPEs were transiently transfected with full-length EGFP-FBP17 (green) and F-Tractin-RFP (f-actin, red), and were fed Alexa Fluor 647 dye-labeled isolated OS. The top and bottom rows of the panels both show selected time-lapse images from movies of separate cells; Movie 5 shows the cell in top row, and Movie 6 shows the cell in the bottom row. In the top row, FBP17 begins to accumulate at the cup rim (i.e., where the membrane folds into an invagination), as it begins to grow over the bound OS (2.7 min). It remains restricted to the rim even as the cup grows (10 min); arrowheads indicate FBP17 at the cup rim. In the bottom row, FBP17 is found at the rim of an already extended cup and remains there even when a phagosome is formed (3.3 min), and travels down the cup and into the cell. When the remaining OS becomes dissociated from the RPE surface, and the cup begins regressing into the cell, FBP17 is no longer localized to the cup. **B**, Primary mouse RPE cells were transiently transfected with the BAR domain of amphiphysin-1 tagged to mCherry (AMPH1-BAR, red) and F-Tractin-GFP (f-actin, green), and fed Alexa Fluor 647 dye-labeled isolated OS. Selected frames from Movie 7 are shown. The AMPH1-BAR domain was enriched at the cup rim, similar to FBP17, but also strongly localized to the base of the cup (white arrowheads). Here, the extended cup (0–2.3 min) regresses back toward the cell surface without fully enveloping the bound OS particle (5.7 min), before attempting to extend over the OS again from 8.3 min onward. During this process, both regions of AMPH1-BAR appear to coalesce. **C**, **D**, Examples of frames from the original fluorescence imaging. **C** shows the fluorescence of the f-actin and FBP17 at the 3.3 min time point in **A**, and **D** shows the fluorescence of f-actin, AMPH1-BAR, and OSs at the 0.7 and 3.7 min time points in **B**. Note that the colors of the f-actin and OSs do not correspond to those in other figures and are also different between the FBP17 and AMPH1-BAR experiments; this is because we only had FBP17 tagged with EGFP and AMPH1-BAR tagged with mCherry.

tissue, suggested either photoreceptor cell autonomous shedding of distal disks (Young, 1971) or scission by the RPE (Spitznas and Hogan, 1970; Steinberg et al., 1977). The literature that followed commonly sided with the former, often stating that the OS tips are shed and then phagocytosed by the RPE, as two distinct events. This view persists in much of the recent literature, although (1) no clear evidence for shed packets of disk membranes in the subretinal space (the extracellular space between the OSs and the RPE) has been shown (Lakkaraju et al., 2020); and (2) it has been demonstrated that normal association of OSs with the RPE is required for removal of disk membranes from the OS tips, with OSs in regions of retinal detachment unable to shed their tips (Williams and Fisher, 1987). Here, our live-cell imaging enabled a temporal analysis of the process and provided complete 3-D views

of labeled f-actin in the phagocytic cup extending around an OS tip. Thus, it was devoid of the ambiguity inherent in 2-D profiles. Imaging showed increased concentrations of labeled actin filaments occurring in the RPE, around the site where the OS tip became separated from the OS. The increased concentration of actin filaments at these sites suggested that dynamic actin filaments in the RPE help to drive the scission event.

Throughout this article, we have used the terms, "phagocytosis" and "phagosome," because of historical usage. Phagocytosis is used in cell biology to describe the ingestion of large particles, in contrast to pinocytosis, in which fluid or macromolecules are taken up into vesicles. However, most commonly, phagocytosis (from "phago," meaning "to devour") describes complete engulfment of a whole cell or piece of debris. Our observations of the
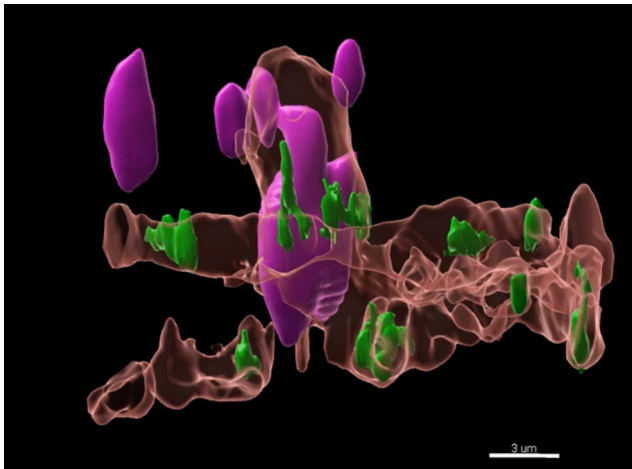
Movie 5. Rendered (Imaris Surfaces) live imaging movie showing the localization of FBP-17 during OS tip ingestion in X–Z profile. OS material is labeled by Alexa 647 dye (magenta), and the RPE cell was transfected with F-Tractin-RFP and pEGFP-C1-FBP17 to show f-actin filaments (reddish-brown) and FBP-17 (green), respectively. The movie plays at 5fps and each frame was acquired every 20 secs over a 10-minute duration, so that the playback rate is 100 times the acquisition rate. FBP-17 localizes predominantly at the cup rim. In this movie, FBP17 accumulation at the rim increases as the cup bound to the OS begins to grow. The upper row of panels in Fig. 7A shows a series of time-lapse images from this movie. [View online]
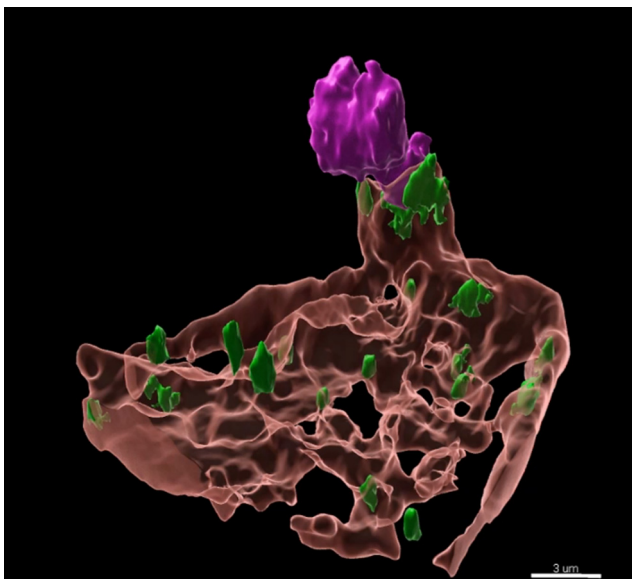
Movie 6. Same as Movie 5, except that it shows a different cell, and later stages of OS tip ingestion. Rendered (Imaris Surfaces) live imaging movies showing the localization of FBP-17 during OS tip ingestion in X–Z profile. OS material is labeled by Alexa 647 dye (magenta), and the RPE cell was transfected with F-Tractin-RFP and pEGFP-C1-FBP17 to show f-actin filaments (reddish-brown) and FBP-17 (green), respectively. The movie plays at 5fps and each frame was acquired every 20 secs over a 10-minute duration, so that the playback rate is 100 times the acquisition rate. FBP-17 localizes predominantly at the cup rim. Note that FBP17 remains at the cup rim even as the ingested OS material descends into the cell. The lower row of panels in Fig. 7A shows a series of time-lapse images from this movie. [View online]

occurrence of scission in the final stage of OS tip ingestion indicate that OS tip ingestion is more akin to trogocytosis (from "trogo," meaning "to nibble"), a related process that involves biting off a piece of a cell, rather than completely engulfing it (Bettadapur et al., 2020). In a review (Freeman and Grinstein, 2021), OS tip ingestion was compared with the trogocytic process

Movie 7. Rendered (Imaris Surfaces) live imaging movie showing the localization of AMPH1-BAR during OS tip ingestion in X–Z profile. OS material is labeled by Alexa Fluor 647 dye (magenta), and the RPE cell was transfected with F-Tractin-GFP and pCAG-AMPH1-BAR-mCherry to show f-actin filaments (green) and FBP-17 (red), respectively. The movie plays at 5 frames/s, and each frame was acquired every 20 s over a 10 min duration, so that the playback rate is 100 times the acquisition rate. AMPH1-BAR localizes to the rim and base of the cup. Figure 7B shows a series of time-lapse images from this movie. [View online]

of synaptic pruning (Weinhard et al., 2018). There are some general parallels between OS ingestion and phagocytosis. For example, the f-actin-based, protruding cup around the OS tip appears to be similar to that shown, also by live-cell imaging, to occur during complement receptor 3-mediated phagocytosis by macrophages (Jaumouillé et al., 2019). However, OS tip ingestion by the RPE shares with trogocytosis the required rupture of the plasma membrane of the target cell; this event makes it fundamentally distinct from phagocytosis by complete engulfment (Vorselen et al., 2020). Hence, trogocytosis provides a more appropriate description of the mechanism of OS tip ingestion.

Although release of the OS tip into the subretinal space has not been observed, changes to the tip of the OS, before detachment, have been reported *in vivo*: a lucifer yellow band, indicating an opening to the extracellular space, near to the tip of frog rod OSs (Matsumoto and Besharse, 1985), and pSIVA labeling of the OS tips in mouse retinas, indicating a localized exposure of PS to the outer leaflet (Ruggiero et al., 2012). These changes may be precursors to OS tip ingestion by the RPE, but they appear to require OS interaction with the RPE (Matsumoto and Besharse, 1985; Ruggiero et al., 2012), indicating that they may be induced by the RPE, or, at the least, they are not controlled autonomously by the photoreceptor cell.

It has been proposed that the extent of the PS exposure defines the size of the ensuing phagosome. Interestingly, the isolated OSs that we fed to our RPE cultures were labeled entirely with pSIVA, indicating PS exposure that was not concentrated at the tip (Fig. 6). Yet, the phagosome size remained comparable to that *in vivo*, only changing in size when actin polymerization had been inhibited with cytochalasin D. Hence, in determining phagosome size, actin dynamics within the RPE cell is not only required, but it also does not seem to be dependent on a PS signal from the OS.

Successive scission events were observed, resulting in multiple OS phagosomes from a single cup. These events may be more common in cell culture conditions, perhaps enhanced by OSs with an altered external PS distribution, as suggested by pSIVA labeling (Fig. 6). Nevertheless, OSs in most animals must yield more than one phagosome each day. For example, a mouse rod OS is ∼25–28 μm long, and 10% of the OS is renewed each day (Besharse and Hollyfield, 1979); given that the diameter of a

phagosome is <2 μm, it follows that a single phagosome from each mouse rod OS would be insufficient to balance the daily renewal rate. Moreover, multiple phagosomes have been reported in the RPE sheaths that surround each cone OS in rhesus monkey and human retinas (Steinberg et al., 1977; Anderson et al., 1978).

Both BAR proteins studied, FBP17 and AMPH1-BAR, were enriched in the region of the membrane cup during OS tip engulfment, suggesting that they assist actin dynamics in the shaping of the membrane cup. Interestingly, there were some differences in the localization of these two BAR proteins. Most notably, while FBP17 quite specifically localized to the cup rim, AMPH1-BAR also localized to the base of the cup and stayed associated with the nascent phagosome until the phagosome moved into the cell. This FBP17 localization, together with the reported preference of FBP17 to associate with intracellular membranes (Stanishneva-Konovalova et al., 2016), suggests that the protein was specifically associated with the membrane of the growing phagocytic cup that is closely apposed to the bound OS. On the other hand, the localization of AMPH1-BAR at the base of the cup suggests a stabilizing role for this N-BAR domain, and the persistent presence of AMPH1-BAR with the nascent phagosome may also be indicative of a structural feature of the membrane surrounding the phagosome. This behavior of AMPH1-BAR appears to contrast that of N-BAR proteins in another study, where the N-BAR proteins were rapidly discarded following scission of the endocytic vesicle, presumably because of the collapse of the highly curved membrane neck at the moment of scission (Taylor et al., 2011).

In conclusion, by live-cell imaging, we have illustrated the ability of the RPE to ingest OS tips as a consequence of f-actin-mediated scission. Also, the shaping of the membrane cup that leads to the scission involves actin dynamics as well as the presence of BAR proteins. The demonstrated live-cell approach offers a way to elucidate the dynamic roles of additional molecular components that may function in particular stages of OS ingestion by the RPE. While our studies have emphasized the role of actin polymerization in the scission of the OS tip, and even its apparent participation in initial movement of the newly ingested tip into the RPE cell, it is likely that some of these processes involve actomyosin contractility. Myosin-2, which is mobilized toward phagocytic cups in the RPE by MERTK and indicated in the OS ingestion process (Strick et al., 2009), and myosin-7a, which associates with early OS phagosomes and is required for their efficient passage through the apical f-actin domain of the RPE (Jiang et al., 2015), represent two actin-based motor proteins that are candidates for actomyosin involvement in OS tip ingestion.

References

Almedawar S, Vafia K, Schreiter S, Neumann K, Khattak S, Kurth T, Ader M, Karl MO, Tsang SH, Tanaka EM (2020) MERTK-dependent ensheathment of photoreceptor outer segments by human pluripotent stem cell-derived retinal pigment epithelium. Stem Cell Rep 14:374–389.

Anderson DH, Fisher SK, Steinberg RH (1978) Mammalian cones: disc shedding, phagocytosis, and renewal. Invest Ophthalmol Vis Sci 17:117–133.

Barger SR, Vorselen D, Gauthier NC, Theriot JA, Krendel M (2022) F-actin organization and target constriction during primary macrophage phagocytosis is balanced by competing activity of myosin-I and myosin-II. Mol Biol Cell 33:br24.

Besharse JC, Hollyfield JG (1979) Turnover of mouse photoreceptor outer segments in constant light and darkness. Invest Ophthalmol Vis Sci 18:1019–1024.

Bettadapur A, Miller HW, Ralston KS (2020) Biting off what can be chewed: trogocytosis in health, infection, and disease. Infect Immun 88:e00930-19.

Bonilha VL, Finnemann SC, Rodriguez-Boulan E (1999) Ezrin promotes morphogenesis of apical microvilli and basal infoldings in retinal pigment epithelium. J Cell Biol 147:1533–1548.

Chaitin MH, Hall MO (1983) The distribution of actin in cultured normal and dystrophic rat pigment epithelial cells during the phagocytosis of rod outer segments. Invest Ophthalmol Vis Sci 24:821–831.

Echarri A, Pavón DM, Sánchez S, García-García M, Calvo E, Huerta-Lopez C, Velazquez-Carreras D, Viaris de Lesegno C, Ariotti N, Lazaro-Carrillo A, Strippoli R, De Sancho D, Alegre-Cebollada J, Lamaze C, Parton RG, Del Pozo MA (2019) An Abl-FBP17 mechanosensing system couples local plasma membrane curvature and stress fiber remodeling during mechanoadaptation. Nat Commun 10:5828.

Esteve-Rudd J, Hazim RA, Diemer T, Paniagua AE, Volland S, Umapathy A, Williams DS (2018) Defective phagosome motility and degradation in cell nonautonomous RPE pathogenesis of a dominant macular degeneration. Proc Natl Acad Sci U S A 115:5468–5473.

Finnemann SC, Bonilha VL, Marmorstein AD, Rodriguez-Boulan E (1997) Phagocytosis of rod outer segments by retinal pigment epithelial cells requires αvβ5 integrin for binding but not for internalization. Proc Natl Acad Sci U S A 94:12932–12937.

Freeman S, Grinstein S (2021) Promoters and antagonists of phagocytosis: a plastic and tunable response. Annu Rev Cell Dev Biol 37:89–114.

Gal A, Li Y, Thompson DA, Weir J, Orth U, Jacobson SG, Apfelstedt-Sylla E, Vollrath D (2000) Mutations in MERTK, the human orthologue of the RCS rat retinal dystrophy gene, cause retinitis pigmentosa. Nat Genet 26:270–271.

Gibbs D, Williams DS (2003) Isolation and culture of primary mouse retinal pigmented epithlelial cells. Adv Exp Med Biol 533:347–352.

Gibbs D, Kitamoto J, Williams DS (2003) Abnormal phagocytosis by retinal pigmented epithelium that lacks myosin VIIa, the Usher syndrome 1B protein. Proc Natl Acad Sci U S A 100:6481–6486.

Hall MO, Abrams T (1987) Kinetic studies of rod outer segment binding and ingestion by cultured rat RPE cells. Exp Eye Res 45:907–922.

Hayer A, Shao L, Chung M, Joubert LM, Yang HW, Tsai FC, Bisaria A, Betzig E, Meyer T (2016) Engulfed cadherin fingers are polarized junctional structures between collectively migrating endothelial cells. Nat Cell Biol 18:1311–1323.

Hazim RA, Williams DS (2018) Cell culture analysis of the phagocytosis of photoreceptor outer segments by primary mouse RPE cells. Methods Mol Biol 1753:63–71.

Itoh T, Erdmann KS, Roux A, Habermann B, Werner H, De Camilli P (2005) Dynamin and the actin cytoskeleton cooperatively regulate plasma membrane invagination by BAR and F-BAR proteins. Dev Cell 9:791–804.

Jaumouillé V, Cartagena-Rivera AX, Waterman CM (2019) Coupling of β2 integrins to actin by a mechanosensitive molecular clutch drives complement receptor-mediated phagocytosis. Nat Cell Biol 21:1357–1369.

Jiang M, Esteve-Rudd J, Lopes VS, Diemer T, Lillo C, Rump A, Williams DS (2015) Microtubule motors transport phagosomes in the RPE, and lack of KLC1 leads to AMD-like pathogenesis. J Cell Biol 210:595–611.

Johnson HW, Schell MJ (2009) Neuronal IP3 3-kinase is an F-actin-bundling protein: role in dendritic targeting and regulation of spine morphology. Mol Biol Cell 20:5166–5180.

Lakkaraju A, Umapathy A, Tan LX, Daniele L, Philp NJ, Boesze-Battaglia K, Williams DS (2020) The cell biology of the retinal pigment epithelium. Prog Retin Eye Res 78:100846.

LaVail MM (1976) Rod outer segment disk shedding in rat retina: relationship to cyclic lighting. Science 194:1071–1074.

Lim JJ, Grinstein S, Roth Z (2017) Diversity and versatility of phagocytosis: roles in innate immunity, tissue remodeling, and homeostasis. Front Cell Infect Microbiol 7:191.

Mao Y, Finnemann SC (2012) Essential diurnal Rac1 activation during retinal phagocytosis requires αvβ5 integrin but not tyrosine kinases focal adhesion kinase or Mer tyrosine kinase. Mol Biol Cell 23:1104–1114.

Matsumoto B, Besharse JC (1985) Light and temperature modulated staining of the rod outer segment distal tips with Lucifer yellow. Invest Ophthalmol Vis Sci 26:628–635.

Matsumoto B, Defoe DM, Besharse JC (1987) Membrane turnover in rod photoreceptors: ensheathment and phagocytosis of outer segment distal tips by pseudopodia of the retinal pigment epithelium. Proc R Soc Lond B Biol Sci 230:339–354.

Mazzoni F, Safa H, Finnemann SC (2014) Understanding photoreceptor outer segment phagocytosis: use and utility of RPE cells in culture. Exp Eye Res 126:51–60.

Nilsson SE (1978) Ultrastructural organization of the retinal pigment epithelium of the Cynomolgus monkey. Acta Ophthalmol (Copenh) 56:883–901.

Notomi S, et al. (2019) Genetic LAMP2 deficiency accelerates the age-associated formation of basal laminar deposits in the retina. Proc Natl Acad Sci U S A 116:23724–23734.

Pikuleva IA, Curcio CA (2014) Cholesterol in the retina: the best is yet to come. Prog Retin Eye Res 41:64–89.

Rakoczy PE, Zhang D, Robertson T, Barnett NL, Papadimitriou J, Constable IJ, Lai CM (2002) Progressive age-related changes similar to age-related macular degeneration in a transgenic mouse model. Am J Pathol 161:1515–1524.

Ruggiero L, Connor MP, Chen J, Langen R, Finnemann SC (2012) Diurnal, localized exposure of phosphatidylserine by rod outer segment tips in wild-type but not Itgb5-/- or Mfge8-/- mouse retina. Proc Natl Acad Sci U S A 109:8145–8148.

Schliwa M (1982) Action of cytochalasin D on cytoskeletal networks. J Cell Biol 92:79–91.

Spitznas M, Hogan MJ (1970) Outer segments of photoreceptors and the retinal pigment epithelium. Interrelationship in the human eye. Arch Ophthalmol 84:810–819.

Stanishneva-Konovalova TB, Kelley CF, Eskin TL, Messelaar EM, Wasserman SA, Sokolova OS, Rodal AA (2016) Coordinated autoinhibition of F-BAR domain membrane binding and WASp activation by Nervous Wreck. Proc Natl Acad Sci U S A 113:E5552–E5561.

Steinberg RH, Wood I, Hogan MJ (1977) Pigment epithelial ensheathment and phagocytosis of extrafoveal cones in human retina. Philos Trans R Soc Lond B Biol Sci 277:459–474.

Strauss O (2005) The retinal pigment epithelium in visual function. Physiol Rev 85:845–881.

Strick DJ, Feng W, Vollrath D (2009) Mertk drives myosin II redistribution during retinal pigment epithelial phagocytosis. Invest Ophthalmol Vis Sci 50:2427–2435.

Taylor MJ, Perrais D, Merrifield CJ (2011) A high precision survey of the molecular dynamics of mammalian clathrin-mediated endocytosis. PLoS Biol 9:e1000604.

Volland S, Esteve-Rudd J, Hoo J, Yee C, Williams DS (2015) A comparison of some organizational characteristics of the mouse central retina and the human macula. PLoS One 10:e0125631.

Vorselen D, Labitigan RLD, Theriot JA (2020) A mechanical perspective on phagocytic cup formation. Curr Opin Cell Biol 66:112–122.

Wavre-Shapton ST, Tolmachova T, Lopes da Silva M, Futter CE, Seabra MC (2013) Conditional ablation of the choroideremia gene causes age-related changes in mouse retinal pigment epithelium. PLoS One 8: e57769.

Weinhard L, di Bartolomei G, Bolasco G, Machado P, Schieber NL, Neniskyte U, Exiga M, Vadisiute A, Raggioli A, Schertel A, Schwab Y, Gross CT (2018) Microglia remodel synapses by presynaptic trogocytosis and spine head filopodia induction. Nat Commun 9:1228.

Williams DS, Fisher SK (1987) Prevention of the shedding of rod outer segment disks by detachment from the retinal pigment epithelium. Invest Ophthalmol Vis Sci 28:184–187.

Williams DS, Shuster TA, Moldrawski MR, Blest AD, Farber DB (1989) Isolation of rod outer segments on Percoll gradients: effect of specific protease inhibition. Exp Eye Res 49:439–444.

Young RW (1967) The renewal of photoreceptor cell outer segments. J Cell Biol 33:61–72.

Young RW (1971) Shedding of discs from rod outer segments in the rhesus monkey. J Ultrastruct Res 34:190–203.

Young RW, Bok D (1969) Participation of the retinal pigment epithelium in the rod outer segment renewal process. J Cell Biol 42:392–403.